Screening the Pathogen Box Compounds for Activity Against *Plasmodium falciparum* Sporozoite Motility

Sachie Kanatani*, Rubayet Elahi, Sukanat Kanchanabhogin, Natasha Vartek, Abhai K. Tripathi, Sean T. Prigge and Photini Sinnis*

W. Harry Feinstone Department of Molecular Microbiology and Immunology, and Johns Hopkins Malaria Research Institute, Johns Hopkins Bloomberg School of Public Health, Baltimore, Maryland, USA

*corresponding authors:
Sachie Kanatani: skanata1@jhu.edu
Photini Sinnis: psinnis1@jhu.edu

Abstract

As the malaria parasite becomes resistant to every drug that we develop, identification and development of novel drug candidates is essential. Many studies have screened compounds designed to target the clinically important blood stages. However, if we are to shrink the malaria map, new drugs that block transmission of the parasite are needed. Sporozoites are the infective stage of the malaria parasite, transmitted to the mammalian host as mosquitoes probe for blood. Sporozoite motility is critical to their ability to exit the inoculation site and establish infection and drug-like compounds targeting motility are effective in blocking infection in the rodent malaria model. In this study, we established a moderate throughput motility assay for sporozoites of the human malaria parasite *Plasmodium falciparum*, enabling us to screen the 400 drug-like compounds from the Pathogen box provided by Medicines for Malaria Venture for their activity. Compounds exhibiting inhibitory effects on *P. falciparum* sporozoite motility were further assessed against transmission-blocking activity and asexual stage growth. Five compounds had a significant inhibitory effect on *P. falciparum* sporozoite motility at 1 μM concentration and four of these compounds also showed significant inhibition on transmission of *P. falciparum* gametocytes to the mosquito and of these four, three had previously been shown to have inhibitory activity on asexual blood stage parasites. Our findings provide new antimalarial drug candidates that have multi-stage activity.

Introduction

Malaria is caused by parasites of the genus *Plasmodium,* transmitted to humans by *Anopheles* mosquitoes. *Plasmodium falciparum* is responsible for the majority of malaria-induced deaths with over 400,000 deaths and more than 200 million people affected

48 annually (1). As *P. falciparum* is increasingly becoming resistant to artemisinin-based
49 combination therapies (2), new drugs are essential. Drugs used to treat malaria target the
50 asexual blood stages of the parasite, which are responsible for all clinical manifestations of
51 malaria. The majority of these drugs have no impact on the transmission stages of the
52 malaria parasite, and in some cases have been found to increase transmission to the
53 mosquito host (3–5). Recently there has been some focus on developing drugs that target
54 both blood stages and transmission stages, a goal that would enable us to work towards
55 malaria elimination as we treat clinical malaria cases.

56 Malaria parasites cycle between mosquito and mammalian hosts. Infection in the
57 mammalian host is initiated when mosquitoes inoculate sporozoites as they probe blood.
58 Sporozoites are actively motile, migrating through the dermis to enter the blood circulation
59 (6), which carries them to the liver. Here they develop into exoerythrocytic stages, which
60 produce thousands of hepatic merozoites that initiate the blood stage of infection. Some
61 blood stage parasites differentiate to gametocytes, which are responsible for transmission
62 back to the mosquito. Upon being ingested during blood feeding, gametocytes develop into
63 gametes, fuse, and ultimately form ookinetes, which migrate across the mosquito gut
64 epithelium and develop into oocysts, where sporozoites are produced. These sporozoites
65 migrate to salivary glands and wait to be inoculated into the next mammalian host. Both
66 transmission to the mammalian host and back to the mosquito are severe bottlenecks for
67 the parasite (7). Thus, targeting these stages with drugs could have significant
68 transmission-blocking potential.

69 Sporozoites move by gliding motility, a substrate-based form of locomotion that does not
70 involve a change in cell shape and is powered by an actin-myosin motor beneath the

sporozoite plasma membrane (8). Gliding motility involves the rapid turnover of surface adhesion sites with secretion of adhesins from the apical end followed by their translocation posteriorly via the actin-myosin motor and their shedding via the activity of a surface rhomboid protease (9, 10). Motility is required for sporozoite exit from the dermal inoculation site and entry into hepatocytes, and thus is an excellent target for intervention. Motility studies have largely been performed using the rodent malaria model (11, 12) since to date, it has been difficult to perform live gliding assays with sporozoites of the human malaria parasite *P. falciparum*. In this study, we developed a moderate-throughput *in vitro* *P. falciparum* sporozoite motility assay and screened the 400 Pathogen Box compounds available from Medicines for Malaria Venture (MMV), which demonstrate activity against a range of different pathogens, predominantly *Mycobacterium* and two groups of eukaryotic protists, the Apicomplexans and Kinetoplastids. Active compounds were further screened against gametocyte transmission to the mosquito and blood stage parasites to identify multi-stage active compounds (Fig. 1A).

Results

Moderate throughput *Plasmodium falciparum* sporozoite motility assay

We began by establishing a motility assay for *P. falciparum* sporozoites. We found that if wells of a 96-well plate were coated with mAb 2A10, specific for the repeat region of the sporozoite's major surface protein, the circumsporozoite protein (CSP), *P. falciparum* sporozoites would adhere to the wells and initiate motility. Unlike rodent malaria sporozoites which will initiate gliding motility on uncoated glass slides, *P. falciparum* sporozoites appear to need the additional adhesive force provided by binding of its surface protein to imobilized antibody in order to glide

in two-dimensional spaces. Sporozoites and the CSP trails they leave behind as they move were visualized by staining for CSP, using biotinylated mAb 2A10 followed by avidin conjugated to a fluorophore. Plates were imaged with a high content imaging system and the area occupied by the trails was quantified using cell profiler software (Fig. 1B). This assay was validated by quantification of motility in the presence of known inhibitors, soluble mAb 2A10 (13) and cytochalasin D, an actin polymerization inhibitor (14). Sporozoites were pre-incubated with 1 µM of each compound and then allowed to move in wells of a glass-bottom plate for 1 h. Treatment with either mAb 2A10 or cytochalasin D inhibited sporozoite motility in a dose-dependent manner (Fig. 1C-F), indicating that this assay allows for moderate-throughput measurement of sporozoite motility.

Screening of pathogen box compounds on *Plasmodium falciparum* sporozoite motility

The pathogen box contains 400 drug-like molecules active against neglected diseases including 125 compounds targeting the blood stages of malaria (https://www.mmv.org/mmv-open/pathogen-box/about-pathogen-box). Screening of the compounds at 1 µM in our sporozoite motility assay demonstrated that five compounds displayed greater than or equal to 50 % inhibition of motility (Sup Fig. 1). We confirmed these results by re-testing the active compounds in 3 biological replicates (Fig. 2A&B). The potency of each compound was then assessed by treating sporozoites with serially diluted compounds from 1 µM to 0.0039 µM. MMV688703 showed the highest potency with significant inhibition at 0.0156 µM and MMV030734 showed second highest potency with significant inhibition at 0.0625 µM (Fig. 2C). The three remaining compounds (MMV688854, MMV687800, and MMV687807) had significant inhibition at 0.25 µM but not at lower concentrations (Fig. 2C). Importantly, the

hepatocyte cytotoxicity data provided by MMV showed that 4 of the 5 compounds did not have significant toxicity to HepG2 cells, while MMV687807 showed some toxicity to HepG2 cells (Table 1). We then determined whether these compounds were directly toxic to parasites, using a viability assay based on a live/dead dye that binds to free amines, resulting in dead cells becoming brightly fluorescent (Fig. 3A). Similar to the motility assay, sporozoites were pre-incubated with compounds at 1 µM and the live/dead dye for 30 minutes followed by a 1 h incubation at 37 °C. Sporozoites were then stained for CSP for visualization purposes. Sporozoites treated with any of the 5 motility-inhibiting compounds were > 90 % viable (Fig. 3B), suggesting that these compounds did not have a direct cytotoxic effect on sporozoites.

Testing the pathogen box inhibitory compounds on *Plasmodium berghei* sporozoite motility

A previous study from the Frischknecht group screened the 400 compounds in the MMV Malaria Box for their impact on sporozoite motility of the rodent malaria parasite *Plasmodium berghei* (11). These compounds are different from those in the MMV Pathogen Box. They found that three of the Malaria Box compounds, MMV665953, MMV665852, and MMV007224, inhibited motility by > 75 %, however, due to toxic effects on hepatocytes, these compounds were not pursued further. To determine if there was cross-species activity of our hits, we tested the active Pathogen Box compounds on *P. berghei* sporozoites. These sporozoites make tighter circles than *P. falciparum* sporozoites complicating quantification of the area occupied by the trails using high content imaging. Thus, we optimized the screening method for *P. berghei* by quantifying stained trails using fluorescence microscopy, measuring total fluorescence intensity using Image J. We verified this assay with mAb 3D11, an inhibitory antibody specific for the *P. berghei* CSP repeats, and cytochalasin D (Fig. 4A&B). As shown, treatment with mAb 3D11 and cytochalasin

D inhibited sporozoite motility in a dose-dependent manner. We then assessed the 5 inhibitory Pathogen Box compounds and all of them showed significant inhibitory effect on *P. berghei* sporozoite motility (Fig. 4C&D). MMV030734 and MMV688703 showed > 70 % inhibition while MMV688854, MMV687807, and MMV687800 were less potent. These findings are similar to the inhibitory activity of these compounds on *P. falciparum* sporozoite motility at 1 µM, with MMV030734 and MMV688703 being the most potent and MMV687800 demonstrating the least inhibitory activity (Fig. 2B). Thus, the rodent model can be used for screening compounds targeting motility, though ultimately compounds need to be screened on human malaria parasites.

Testing the pathogen box inhibitory compounds in transmission blocking assays

We next determined whether any of our active compounds had inhibitory activity on transmission of *Plasmodium* parasites to the mosquito. To do this we added each of the 5 compounds at 1 µM to the *P. falciparum* gametocyte-blood meal fed to mosquitoes. Nine days later, mosquito midguts were dissected and oocyst numbers were counted (Fig. 5A&B). We performed this assay using two different gametocyte concentrations, 0.1% and 0.03% of total erythrocytes. As shown in Fig. 5C, when fed on blood containing low gametocyte counts, there was a significant reduction in oocyst number in mosquitoes fed with four of the compounds, MMV030734, MMV688854, MMV687800, and MMV688703. By contrast, when mosquitoes were fed on blood with higher gametocyte counts, only MMV030734 and MMV68854 had inhibitory activity on transmission. One compound, MMV687807 had no effect on transmission even when blood contained low gametocyte numbers (Fig. 5C and 5D).

Asexual blood stage parasites treated with MMV030734 exhibit egress defects

Though these compounds had been previously tested against asexual blood stage parasites of *P. falciparum* in a high-throughput assay (15), we wanted to confirm these results for the two compounds (MMV030734 and MMV688854) that had strong inhibitory activity on both transmission stages (Fig. 6A). Synchronized *P. falciparum* ring stage parasites were grown in the presence of 1 μM MMV030734 or MMV688854 or 0.1% DMSO for 60 hours. At the end of the experiment, Giemsa-stained blood smears were made and ring stage parasites were counted. MMV688854 had no impact on parasite growth, however, no ring stage parasites were observed in the culture treated with MMV030734 (Fig. 6B). Interestingly, the Giemsa-stained slides from the MMV030734-treated culture showed that parasite growth was halted at the schizont stage, suggesting an egress defect (Fig. 6C). To confirm this we counted ring, trophozoite, and schizont stage of parasites in infected cells. As shown in Fig. 6D, all parasites were at the schizont stage in the culture treated with MMV030734 while majority of the population in the culture treated with MMV688854 and the DMSO control was ring stage parasites. To further characterize MMV030734, we determined its half-maximal effective concentration (EC_{50}) and found that its inhibitory activity on blood stage parasite growth was in the nanomolar range (Fig. 6E).

Discussion

In this study, we have established a quantitative, moderate-throughput assay of *P. falciparum* sporozoite motility and used it to screen 400 drug-like compounds targeting neglected diseases. Five compounds had a significant inhibitory effect on *P. falciparum* sporozoite motility: MMV688854, MMV687800, MMV687807, MMV688703, and

MMV030734 (Sup Fig. 1 and Fig. 2). These 5 compounds were further assessed in *P. falciparum* transmission blocking assays and two of them, MMV030734 and MMV688854, had strong inhibitory activity on transmission to the mosquito while two others, MMV687800 and MMV688703, had moderate activity in this assay (Fig. 5). Three of the compounds that had dual transmission-blocking activity, MMV030734, MMV687800, MMV688703, had been previously shown to inhibit growth of *P. falciparum* asexual stage parasites (15), with our study extending the findings with MMV030734 demonstrating an effect on egress from infected erythrocytes (Fig. 6). When the 5 motility-inhibitory compounds were tested in motility assays with the rodent malaria parasite *P. berghei*, all 5 compounds demonstrated inhibitory activity, with MMV030734 and MMV688703 having the greatest inhibitory activity in both species, highlighting the conservation of the gliding motility machinery across the genus, and the usefulness of the rodent model in testing compounds targeting motility.

Interestingly, three of the compounds, MMV688703, MV030734, and MMV688854, are known to target protein kinases (Table 1). MMV688703, a substituted pyrrole, is also known as Compound 1, a cGMP-dependent protein kinase (PKG) inhibitor in *Toxoplasma gondii and Eimeria tenella* (16, 17), MMV030734, a trisubstituted imidazole, binds to *P. falciparum* calcium-dependent protein kinase 1 (PfCDPK1) (18) and inhibits blood stage parasites, and MMV688854, a pyrazolopyrimidine bumped kinase inhibitor derivative, is a known inhibitor of *Toxoplasma gondii* CDPK1 (TgCDPK1) (19, 20). The other compounds that had inhibitory effect on sporozoite motility were MMV687800 and MMV687807, both of which have anti-mycobacterial activity. MMV687800 is Clofazimine, which is used

209 together with dapsone to treat leprosy. Though its precise mechanism of action is unclear,
210 clofazimine interacts with bacterial membrane phospholipids and interferes with K^+ uptake
211 and ATP production (21). MMV687807 is a salicylanilide-derivative with significant
212 cytotoxicity (22). There are also 26 reference compounds in the pathogen box and of these,
213 doxycycline, primaquine, amphotericin B, and bedaquiline had significant inhibitory
214 activity against asexual blood stages (15), however they had no impact on sporozoite
215 motility (Sup Fig. 1).
216
217 Among the five compounds that inhibited sporozoite motility, MMV688703 or Compound 1,
218 had the greatest potency, with activity in the low nanomolar range. This inhibitor also had
219 activity in blocking parasite transmission to the mosquito. The compound's target molecule,
220 PKG, is likely the sole mediator of cGMP signaling in *Plasmodium* parasites with
221 phosphoproteomic studies showing hundreds of downstream substrates (23 and reviewed
222 in 22). Thus it is not surprising that PKG regulates many cellular processes in *Plasmodium*,
223 including egress from red blood cells, gamete formation, and motility (25–28). The critical
224 role of PKG in cellular pathways occurring across the life cycle in both mosquito and
225 mammalian hosts, can be explained by the recent demonstration that PKG controls
226 cytosolic Ca^{2+} levels which in turn regulate a variety of stage-specific effector pathways. Its
227 role in motility has been demonstrated in *P. berghei*, where its been shown to inhibit the
228 regulated secretion of micronemes, a calcium-dependent process necessary for gliding
229 motility, and phosphorylation of central components of the actin-myosin motor (28, 29).
230 Our current findings demonstrate that PKG signaling is critical for motility in *P. falciparum*.
231 Additionally, the modest but significant transmission blocking activity of MMV688703

extends previous findings with this compound on gametogenesis and ookinete motility to show that these defects impact mosquito transmission**.** Taken together these data, covering a wide range of phenotypic assays in both human and rodent malaria parasites, make a compelling case that targeting PKG could have potent multi-stage activity.

Interestingly, the two compounds that had strong transmission-blocking activity in addition to their inhibitory activity on sporozoite motility were MMV688854 and MMV030734, which target kinases of the CDPK family (18–20). CDPKs are serine/threonine protein kinases that are mediators of calcium signaling in *Plasmodium* and other Apicomplexa (30, 31), containing calcium-binding EF hand domains that when bound to Ca^{2+} led to conformational changes, which enable them to rapidly respond to Ca^{2+} fluxes. Apicomplexan parasites have multiple CDPK family members, with *P. falciparum* having 7 CDPKs and the rodent malaria parasites having orthologs to all but one of these. Toxoplasma CDPK1, the target of MMV688854, has been shown to regulate microneme secretion and inhibition of TgCDPK1 results in blockade of parasite motility, host cell invasion, and egress from host cells (32). The *Plasmodium* ortholog of TgCDPK1 is CDPK4. Studies with *P. berghei* demonstrated a role for CDPK4 in sporozoite gliding motility and hepatocyte invasion (29, 33) and in both *P. berghei* and *P. falciparum*, CDPK4 controls microgametocyte activation and exflagellation (34–36). MMV030734 has been shown to target PfCDPK1 which is expressed throughout the *Plasmodium* life cycle, phosphorylates motor complex proteins such as myosin A tail domain-interacting protein (MTIP) and glideosome associated protein 45 (GAP45) (37) consistent with the recent demonstration in *P. berghei* that it plays a critical role in sporozoite motility and invasion (33).

Furthermore, deletion of PfCDPK1 results in slower growth of asexual blood stages and the formation of gametocytes that are not infectious to mosquitoes (38). Recently, the trisubstituted imidazole MMV030084, which is an analogue of MMV030734, has been identified as multi-stage targeting compound, inhibiting *P. berghei* liver stage, *P. falciparum* asexual blood stage development, and male gamete activity (39). Using a chemoproteomics approach, they found that MMV030084 targeted both PfCDPK1 and PKG, however, conditional knockdown and molecular modeling studies pointed to PKG as being the primary target (39).

Our finding that three of the dual-transmission blocking compounds target either PKG or the CDPK family of kinases highlight the central role of calcium signaling as *Plasmodium* parasites move between their mammalian and mosquito hosts and support the idea that PKG, the master regulator of parasite Ca^{2+} levels, and the CDPKs, the effectors of calcium signaling (24, 29, 40), are excellent targets for multi-stage inhibitory drugs. Our new moderate-throughput screening strategy for sporozoite motility facilitates compound testing on *P. falciparum* pre-erythrocytic stages and future work on identifying transmission-blocking compounds and pre-erythrocytic stage vaccine candidates.

Materials and Methods

Ethics statement

All animal work was conducted in accordance with the recommendations in the Guide for the Care and Use of Laboratory Animals of the National Institutes of Health. The protocol was approved by the Johns Hopkins University Animal Care and Use Committee (Protocol

278 #M017H325), which is fully accredited by Association for Assessment and Accreditation of
279 Laboratory Animal Care.
280
281 **Mosquito infection with *P. falciparum* NF54**
282 Mosquito infection with *P. falciparum* NF54 was performed as previously described (41).
283 Asexual cultures were maintained *in vitro* in O^+ erythrocytes at 4% hematocrit in RPMI 1640
284 (Corning) supplemented with 74 μM hypoxanthine (Sigma), 0.21% sodium bicarbonate (Sigma),
285 and 10% v/v heat inactivated human serum. Cultures were maintained at 37°C in a candle jar
286 made from glass desiccators. Gametocyte cultures were initiated at 0.5% parasitemia and at 4%
287 hematocrit. Medium was changed daily for up to 15 to 18 days without the addition of fresh
288 blood to promote gametocytogenesis. Adult *Anopheles stephensi* mosquitoes (3-7 days post-
289 emergence) were allowed to feed through a glass membrane feeder for up to 30 minutes
290 on gametocyte cultures in 40% hematocrit containing fresh O^+ human serum and O^+ erythrocytes.
291 Infected mosquitoes were maintained for up to 19 days at 25°C and 80% humidity and were
292 provided with 10% sucrose solution.
293
294 **Mosquito infection with *P. berghei* WT-ANKA**
295 Mosquito infection with *P. berghei* WT-ANKA was performed as previously described (42).
296 Swiss Webster mice (Taconic) were infected with *P. berghei* ANKA wild-type parasites and
297 once abundant gametocyte stage parasites were observed, *An. stephensi* mosquitoes (3-7 days
298 post-emergence) were allowed to feed on infected mice. Infected mosquitoes were maintained
299 for up to 25 days at 18°C and 80% humidity and were provided with 10% sucrose solution.
300

Pathogen box compounds

Pathogen box compounds were obtained from the Medicines for Malaria Venture (MMV) and consisted of 400 compounds at 10 mM concentration, dissolved in dimethyl sulfoxide (DMSO, Sigma). Compounds were diluted to 1 mM in DMSO and aliquoted into 96 well storage micro-plates (Sigma, CLS3363) and stored at -80°C.

P. falciparum moderate-throughput sporozoite motility assay

15,000 freshly dissected *P. falciparum* salivary gland sporozoites in 60 µl of 2% bovine serum albumin (BSA) in Hank´s Balanced Salt Solution (HBSS) at pH 7.4 were mixed with 60 µl of each pathogen box compound at 2 µM which and added to a well of a U-bottom 96 well plate (Falcon, 353077). The final concentration of each pathogen box compound was at 1 µM in 1% BSA in HBSS. The plate was incubated for 30 minutes at 20°C and sporozoites and compound mixture were transferred to a 96 well glass bottom plate (Griner, 655892) coated with 5 µg/ml of mAb 2A10 in PBS. The plate was centrifuged for 3 minutes at 300 × g and incubated for 1 h at 37°C. Wells were fixed in 4% paraformaldehyde in PBS, blocked with 1% BSA in PBS (pH 7.4) and stained with biotinylated mAb 2A10 in 1% BSA in PBS (pH 7.4) for 1 h at room temperature, followed by detection with Alexa Fluor 488 streptavidin (Invitrogen, S11223) diluted at 1:500 in PBS for 1 h at room temperature. Samples were preserved in a glycerol / PBS solution (ratio, 9:1) at 4°C and the plate was imaged within one week. Imaging was performed on 25 positions per well (5 x 5, 500 µm apart) by using ImageXpress Micro XLS Widefield high-content analysis system (Molecular Devices) with 40X Plan fluor objective.

Quantification of area occupied by trails using Cell Profiler software

Image analysis was automated with the open source Cell Profiler software (version 3.0.0) (43). All images were run through a pipeline designed to threshold the images and quantify area occupied by trails. Image intensity was rescaled from 0 - 0.007 to 0 – 1 and the rescaled image was used to set the threshold which was set automatically by using the minimum cross entropy set up in the Cell Profiler pipeline. Following this, object pixel diameter size between 5 to 1,000 was counted and exported to an excel file.

Testing pathogen box compounds on *P. berghei* sporozoite motility

Coverslips were placed in 24-well plates and coated with 5 µg/ml of mAb 3D11 in PBS for 1 h at room temperature and then washed. A total of 50,000 sporozoites in HBSS with 2% BSA (pH 7.4) were mixed with pathogen box compounds, cytochalasin D or mAb 3D11 in a low retention 1.5 ml tube (Axygen, MCT-175-L-C) and pre-incubated for 30 minutes at 20°C. Each sporozoite and compound mixture was then added to an mAb 3D11-coated well, centrifuged onto the coverslip for 3 minutes at 300 × g and incubated for 1 h at 37°C. Wells were fixed in 4% paraformaldehyde in PBS, blocked in 1% BSA in PBS (pH 7.4) and stained with biotinylated mAb 3D11 diluted at 1:500 in 1% BSA in PBS (pH 7.4) for 1 h at room temperature, followed by detection with Alexa Fluor 488 streptavidin (Invitrogen) diluted at 1:500 in PBS for 1 h at room temperature. Samples were mounted in gold antifade mountant (Invitrogen, P36935) and imaged with fluorescence microscopy (Nikon E600) using 40X objective. Twenty-five positions per slide were acquired using identical exposure settings and acquired images were batch processed using Fiji (https://fiji.sc/) to measure total fluorescence intensity.

Sporozoite viability assessment

20,000 freshly dissected sporozoites were pre-incubated with pathogen box compounds at 1 µM concentration and 1:1,000 diluted live/dead fixable green stain (Invitrogen, L23101) in HBSS with 1% BSA (pH 7.4) at 20°C for 30 minutes and then transferred to 48 well plate containing a coverslip, centrifuged at 300 × g for 3 minutes and further incubated at 37°C for 1 h, to replicate the treatment of sporozoites in the gliding assay. After incubation, sporozoites were fixed with 4% PFA, blocked with 1% BSA in PBS (pH 7.4) and stained with 1 µg/ml of mAb 2A10 in 1% BSA in PBS (pH 7.4) followed by detection with Alexa fluor 594 goat anti-mouse secondary antibody (Invitrogen, A11032). Samples were mounted in gold antifade mountant (Invitrogen) and observed by fluorescence microscopy. For each condition, 100 sporozoites were identified by CSP staining (red) and dead sporozoites were counted by live/dead stain (green) to quantify viability.

Testing pathogen box compounds using the standard membrane feeding assay (SMFA)

The pathogen box compounds (MMV030734, MMV688854, MMV687800, MMV687807, MMV688703) or DMSO in HBSS were mixed with gametocyte cultures such that compound final concentration was at 1 µM and DMSO was at 0.1% and fed to adult female *An. stephensi* mosquitoes (3-7 days post-emergence). Cultures with final gametocytemias of 0.3% and 0.01% were used for feeding. *An. stephensi* mosquitoes were allowed to feed for up to 30 minutes. Infected mosquitoes were maintained at 25°C and 80% humidity and were provided with 10% sucrose solution. Oocyst development was quantified on day 9 post blood feeding by staining mosquito midguts with 0.1% mercurochrome (Sigma, M7011) in PBS and counting by bright-field microscopy with a 10X objective.

370 **Testing pathogen box compounds on *Plasmodium falciparum* asexual stages**

371 The *P. falciparum* transgenic NF54^{attB} line (44) which has similar EC_{50} of chloroquine to NF54
372 wild type (45, 46) were cultured in O^+ erythrocytes at 2% hematocrit and maintained in 25 cm^2
373 gassed flasks (94% N_2, 3% O_2, and 3% CO_2) at 37°C. The cultures were kept in RPMI 1640
374 medium with L-glutamine (US Biological, R8999) supplemented with 20 mM HEPES, 0.2%
375 sodium bicarbonate, 12.5 µg/mL hypoxanthine, 5 g/L Albumax II (Life Technologies, S7563),
376 and 25 µg/mL gentamicin. Cultures were synchronized using 5% (wt/vol) sorbitol as previously
377 outlined (47) and synchronized ring parasites were seeded at 1% parasitemia and 1% hematocrit
378 and treated with 1 µM of the indicated pathogen box compounds or 0.1% DMSO or 1 µM
379 chloroquine for 60 hours. After incubation at 37°C for 60 h, parasite growth was quantified by
380 Giemsa-stained blood smear. To determine the half-maximal effective concentration (EC_{50}) of
381 MMV030734, sorbitol-synchronized ring parasites were seeded at 3% parasitemia and 2%
382 hematocrit in a 96-well flat bottom plate and grown in the presence of inhibitor at 37°C for 72 h.
383 A concentration series for MMV030734 (17 pM to 3 µM) and chloroquine (487 pM to 250 nM)
384 was tested. After 72 h, parasite growth was quantified using SYBR Green I (Invitrogen) to stain
385 DNA and an Attune NxT Flow Cytometer as described previously (48, 49). Parasitemia from
386 the MMV030734 and chloroquine samples were normalized to the 0.1% DMSO control. Data
387 from two independent biological replicates, each with four technical replicates, were fit to a four-
388 parameter sigmoidal dose-response curve using Prism V8.4 (version 8.4, GraphPad).
389
390 **Statistical analysis**
391 All statistical analyses were performed with Graphpad Prism (Version 7 or 8.4).
392

Acknowledgements

We would like to thank the team of the parasitology and insectary core facilities at the Johns Hopkins Malaria Research Institute, the Johns Hopkins School of Medicine Microscopy Facility (MicFac) and Hoku West-Foyle for invaluable assistance. This work was supported by the National Institutes of Health (R01 AI132359 to PS, R01 AI065853 to STP), Johns Hopkins Malaria Research Institute postdoctoral fellowships (SK and RE), Bloomberg Family Philanthropies, and NIH grants that funded the MicFac high content imager (R01GM28007-S1 and R01GM66817-S1).

References

1. World Health Organization. World Malaria Report 2020.
2. Ariey F, Witkowski B, Amaratunga C, Beghain J, Langlois AC, Khim N, Kim S, Duru V, Bouchier C, Ma L, Lim P, Leang R, Duong S, Sreng S, Suon S, Chuor CM, Bout DM, Ménard S, Rogers WO, Genton B, Fandeur T, Miotto O, Ringwald P, Le Bras J, Berry A, Barale JC, Fairhurst RM, Benoit-Vical F, Mercereau-Puijalon O, Ménard D. 2014. A molecular marker of artemisinin-resistant Plasmodium falciparum malaria. Nature 505:50–55.
3. Bousema T, Okell L, Shekalaghe S, Griffin JT, Omar S, Sawa P, Sutherland C, Sauerwein R, Ghani AC, Drakeley C. 2010. Revisiting the circulation time of Plasmodium falciparum gametocytes: molecular detection methods to estimate the duration of gametocyte carriage and the effect of gametocytocidal drugs. Malar J 9:136.
4. Hogh B, Gamage-Mendis A, Butcher GA, Thompson R, Begtrup K, Mendis C, Enosse SM, Dgedge M, Barreto J, Eling W, Sinden RE. 1998. The differing impact of chloroquine and pyrimethamine/sulfadoxine upon the infectivity of malaria species to the mosquito vector. Am J Trop Med Hyg 58:176–182.
5. Buckling A, Ranford-cartwright LC, Miles A, Read AF. 1999. Chloroquine increases Plasmodium falciparum gametocytogenesis in Vitro. Parasitology 118:339–346.
6. Hopp CS, Chiou K, Ragheb DRT, Salman AM, Khan SM, Liu AJ, Sinnis P. 2015. Longitudinal analysis of Plasmodium sporozoite motility in the dermis reveals component of blood vessel recognition. Elife 4.
7. Graumans W, Jacobs E, Bousema T, Sinnis P. 2020. When Is a Plasmodium-Infected Mosquito an Infectious Mosquito? Trends Parasitol 36:705–716.
8. Baum J, Papenfuss AT, Baum B, Speed TP, Cowman AF. 2006. Regulation of apicomplexan actin-based motility. Nat Rev Microbiol 4:621–628.
9. Ejigiri I, Ragheb DRT, Pino P, Coppi A, Bennett BL, Soldati-Favre D, Sinnis P. 2012. Shedding of TRAP by a Rhomboid Protease from the Malaria Sporozoite Surface Is

Essential for Gliding Motility and Sporozoite Infectivity. PLoS Pathog 8:e1002725.
10. Münter S, Sabass B, Selhuber-Unkel C, Kudryashev M, Hegge S, Engel U, Spatz JP, Matuschewski K, Schwarz US, Frischknecht F. 2009. Plasmodium Sporozoite Motility Is Modulated by the Turnover of Discrete Adhesion Sites. Cell Host Microbe 6:551–562.
11. Douglas RG, Reinig M, Neale M, Frischknecht F. 2018. Screening for potential prophylactics targeting sporozoite motility through the skin. Malar J 17:1–10.
12. Kortagere S, Welsh WJ, Morrisey JM, Daly T, Ejigiri I, Sinnis P, Vaidya AB, Bergman LW. 2010. Structure-based Design of Novel Small-Molecule Inhibitors of Plasmodium falciparum. J Chem Inf Model 50:840–849.
13. Stewart MJ, Nawrot RJ, Schulman S, Vanderberg JP. 1986. Plasmodium berghei sporozoite invasion is blocked in vitro by sporozoite-immobilizing antibodies. Infect Immun 51:859–864.
14. Dobrowolski JM, Sibley LD. 1996. Toxoplasma invasion of mammalian cells is powered by the actin cytoskeleton of the parasite. Cell 84:933–939.
15. Duffy S, Sykes ML, Jones AJ, Shelper TB, Simpson M, Lang R, Poulsen SA, Sleebs BE, Avery VM. 2017. Screening the medicines for malaria venture pathogen box across multiple pathogens reclassifies starting points for open-source drug discovery. Antimicrob Agents Chemother 61:1–22.
16. Diaz CA, Allocco J, Powles MA, Yeung L, Donald RGK, Anderson JW, Liberator PA. 2006. Characterization of Plasmodium falciparum cGMP-dependent protein kinase (PfPKG): Antiparasitic activity of a PKG inhibitor. Mol Biochem Parasitol 146:78–88.
17. Gurnett AM, Liberator PA, Dulski PM, Salowe SP, Donald RGK, Anderson JW, Wiltsie J, Diaz CA, Harris G, Chang B, Darkin-Rattray SJ, Nare B, Crumley T, Blum PS, Misura AS, Tamas T, Sardana MK, Yuan J, Biftu T, Schmatz DM. 2002. Purification and molecular characterization of cGMP-dependent protein kinase from Apicomplexan parasites. A novel chemotherapeutic target. J Biol Chem 277:15913–15922.
18. Crowther GJ, Hillesland HK, Keyloun KR, Reid MC, Lafuente-Monasterio MJ, Ghidelli-Disse S, Leonard SE, He P, Jones JC, Krahn MM, Mo JS, Dasari KS, Fox AMW, Boesche M, Bakkouri M El, Rivas KL, Leroy D, Hui R, Drewes G, Maly DJ, Van Voorhis WC, Ojo KK. 2016. Biochemical screening of five protein kinases from plasmodium falciparum against 14,000 Cell-Active compounds. PLoS One 11:1–16.
19. Johnson SM, Murphy RC, Geiger JA, Derocher AE, Zhang Z, Ojo KK, Larson ET, Perera BGK, Dale EJ, He P, Reid MC, Fox AMW, Mueller NR, Merritt EA, Fan E, Parsons M, Van Voorhis WC, Maly DJ. 2012. Development of Toxoplasma gondii calcium-dependent protein kinase 1 (Tg CDPK1) inhibitors with potent anti- toxoplasma activity. J Med Chem 55:2416–2426.
20. Zhang Z, Ojo KK, Vidadala R, Huang W, Geiger JA, Scheele S, Choi R, Reid MC, Keyloun KR, Rivas K, Kallur Siddaramaiah L, Comess KM, Robinson KP, Merta PJ, Kifle L, Hol WGJ, Parsons M, Merritt EA, Maly DJ, Verlinde CLMJ, Van Voorhis WC, Fan E. 2014. Potent and selective inhibitors of CDPK1 from T. Gondii and C. Parvum based on a 5-aminopyrazole-4-carboxamide scaffold. ACS Med Chem Lett 5:40–44.
21. Cholo MC, Steel HC, Fourie PB, Germishuizen WA, Anderson R. 2012. Clofazimine: Current status and future prospects. J Antimicrob Chemother 67:290–298.
22. Lee IY, Gruber TD, Samuels A, Yun M, Nam B, Kang M, Crowley K, Winterroth B, Boshoff HI, Barry CE. 2013. Structure-activity relationships of antitubercular salicylanilides consistent with disruption of the proton gradient via proton shuttling.

Bioorganic Med Chem 21:114–126.

23. Rotella D, Siekierka J, Bhanot P. 2021. Plasmodium falciparum cGMP-Dependent Protein Kinase – A Novel Chemotherapeutic Target. Front Microbiol 11:1–7.
24. Alam MM, Solyakov L, Bottrill AR, Flueck C, Siddiqui FA, Singh S, Mistry S, Viskaduraki M, Lee K, Hopp CS, Chitnis CE, Doerig C, Moon RW, Green JL, Holder AA, Baker DA, Tobin AB. 2015. Phosphoproteomics reveals malaria parasite Protein Kinase G as a signalling hub regulating egress and invasion. Nat Commun 6.
25. Dvorin JD, Martyn DC, Patel SD, Grimley JS, Collins CR, Hopp CS, Bright AT, Westenberger S, Winzeler E, Blackman MJ, Baker DA, Wandless TJ, Duraisingh MT. 2010. A plant-like kinase in plasmodium falciparum regulates parasite egress from erythrocytes. Science (80-) 328:910–912.
26. Taylor HM, McRobert L, Grainger M, Sicard A, Dluzewski AR, Hopp CS, Holder AA, Baker DA. 2010. The malaria parasite cyclic GMP-dependent protein kinase plays a central role in blood-stage schizogony. Eukaryot Cell 9:37–45.
27. McRobert L, Taylor CJ, Deng W, Fivelman QL, Cummings RM, Polley SD, Billker O, Baker DA. 2008. Gametogenesis in malaria parasites is mediated by the cGMP-dependent protein kinase. PLoS Biol 6:1243–1252.
28. Moon RW, Taylor CJ, Bex C, Schepers R, Goulding D, Janse CJ, Waters AP, Baker DA, Billker O. 2009. A cyclic GMP signalling module that regulates gliding motility in a malaria parasite. PLoS Pathog 5.
29. Govindasamy K, Jebiwott S, Jaijyan DK, Davidow A, Ojo KK, Van Voorhis WC, Brochet M, Billker O, Bhanot P. 2016. Invasion of hepatocytes by Plasmodium sporozoites requires cGMP-dependent protein kinase and calcium dependent protein kinase 4. Mol Microbiol 102:349–363.
30. Ward P, Equinet L, Packer J, Doerig C. 2004. Protein kinases of the human malaria parasite Plasmodium falciparum: The kinome of a divergent eukaryote. BMC Genomics 5:1–19.
31. Harper JF, Harmon A. 2005. Plants, symbiosis and parasites: A calcium signalling connection. Nat Rev Mol Cell Biol 6:555–566.
32. Lourido S, Shuman J, Zhang C, Shokat KM, Hui R, Sibley LD. 2010. Calcium-dependent protein kinase 1 is an essential regulator of exocytosis in Toxoplasma. Nature 465:359–362.
33. Govindasamy K, Bhanot P. 2020. Overlapping and distinct roles of CDPK family members in the pre-erythrocytic stages of the rodent malaria parasite, Plasmodium berghei. PLoS Pathog 16:1–22.
34. Billker O, Dechamps S, Tewari R, Wenig G, Franke-Fayard B, Brinkmann V. 2004. Calcium and a calcium-dependent protein kinase regulate gamete formation and mosquito transmission in a malaria parasite. Cell 117:503–514.
35. Ojo KK, Pfander C, Mueller NR, Burstroem C, Larson ET, Bryan CM, Fox AMW, Reid MC, Johnson SM, Murphy RC, Kennedy M, Mann H, Leibly DJ, Hewitt SN, Verlinde CLMJ, Kappe S, Merritt EA, Maly DJ, Billker O, Van Voorhis WC. 2012. Transmission of malaria to mosquitoes blocked by bumped kinase inhibitors. J Clin Invest 122:2301–2305.
36. Fang H, Klages N, Baechler B, Hillner E, Yu L, Pardo M, Choudhary J, Brochet M. 2017. Multiple short windows of calcium-dependent protein kinase 4 activity coordinate distinct cell cycle events during Plasmodium gametogenesis. Elife 6:1–23.

37. Green JL, Rees-Channer RR, Howell SA, Martin SR, Knuepfer E, Taylor HM, Grainger M, Holder AA. 2008. The motor complex of Plasmodium falciparum: Phosphorylation by a calcium-dependent protein kinase. J Biol Chem 283:30980–30989.
38. Bansal A, Molina-Cruz A, Brzostowski J, Liu P, Luo Y, Gunalan K, Li Y, Ribeiro JMC, Miller LH. 2018. PfCDPK1 is critical for malaria parasite gametogenesis and mosquito infection. Proc Natl Acad Sci U S A 115:774–779.
39. Vanaerschot M, Murithi JM, Pasaje CFA, Ghidelli-Disse S, Dwomoh L, Bird M, Spottiswoode N, Mittal N, Arendse LB, Owen ES, Wicht KJ, Siciliano G, Bösche M, Yeo T, Kumar TRS, Mok S, Carpenter EF, Giddins MJ, Sanz O, Ottilie S, Alano P, Chibale K, Llinás M, Uhlemann AC, Delves M, Tobin AB, Doerig C, Winzeler EA, Lee MCS, Niles JC, Fidock DA. 2020. Inhibition of Resistance-Refractory P. falciparum Kinase PKG Delivers Prophylactic, Blood Stage, and Transmission-Blocking Antiplasmodial Activity. Cell Chem Biol 27:806-816.e8.
40. Fang H, Gomes AR, Klages N, Pino P, Maco B, Walker EM, Zenonos ZA, Angrisano F, Baum J, Doerig C, Baker DA, Billker O, Brochet M. 2018. Epistasis studies reveal redundancy among calcium-dependent protein kinases in motility and invasion of malaria parasites. Nat Commun 9:1–14.
41. Tripathi AK, Mlambo G, Kanatani S, Sinnis P, Dimopoulos G. 2020. Plasmodium falciparum gametocyte culture and mosquito infection through artificial membrane feeding. J Vis Exp 2020:1–23.
42. Vanderberg JP, Gwadz RW. 1980. The Transmission by Mosquitoes of Plasmodia in the Laboratory. Pathology, Vector Studies, and Culture. Academic Press, New York.
43. Lamprecht MR, Sabatini DM, Carpenter AE. 2007. CellProfiler^{TM}: Free, versatile software for automated biological image analysis. Biotechniques 42:71–75.
44. Adjalley SH, Johnston GL, Li T, Eastman RT, Ekland EH, Eappen AG, Richman A, Sim BKL, Lee MCS, Hoffman SL, Fidock DA. 2011. Quantitative assessment of Plasmodium falciparum sexual development reveals potent transmissionblocking activity by methylene blue. Proc Natl Acad Sci U S A 108.
45. Wittlin S, Ekland E, Craft JC, Lotharius J, Bathurst I, Fidock DA, Fernandes P. 2012. in vitro and in vivo activity of solithromycin (CEM-101) against plasmodium species. Antimicrob Agents Chemother 56:703–707.
46. Rahbari M, Rahlfs S, Przyborski JM, Schuh AK, Hunt NH, Fidock DA, Grau GE, Becker K. 2017. Hydrogen peroxide dynamics in subcellular compartments of malaria parasites using genetically encoded redox probes. Sci Rep 7:1–13.
47. Lambros C, Vandenberg JP. 1979. Synchronization of Plasmodium falciparum Erythrocytic Stages in Culture. J Parasitol 65:418–420.
48. Swift RP, Rajaram K, Liu HB, Dziedzic A, Jedlicka AE, Roberts AD, Matthews KA, Jhun H, Bumpus NN, Tewari SG, Wallqvist A, Prigge ST. 2020. A mevalonate bypass system facilitates elucidation of plastid biology in malaria parasites. PLoS Pathog 16:1–26.
49. Tewari SG, Kwan B, Elahi R, Rajaram K, Reifman J, Prigge ST, Vaidya AB, Wallqvist A. 2022. Metabolic adjustments of blood-stage Plasmodium falciparum in response to sublethal pyrazoleamide exposure. Sci Rep 12:1–14.

Figure 1

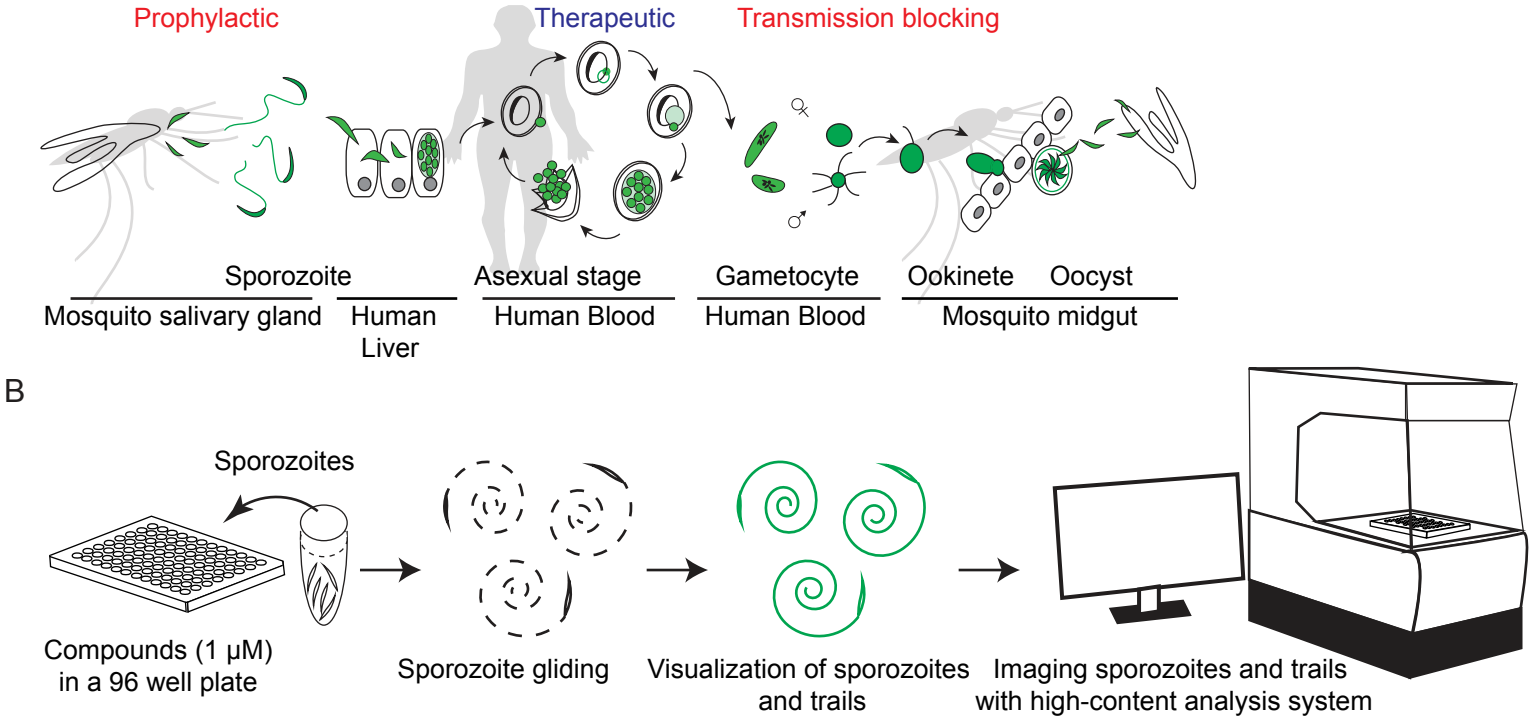

Figure 1. Pathogen box screening strategy and validation.
(A) Pathogen box screening on different *Plasmodium* life cycle stages. Pathogen box compounds were initially screened for their impact on *P. falciparum* sporozoite motility, which is essential for establishing infection in a human host. Compounds with inhibitory effect on sporozoite motility were further assessed on gametocyte to oocyst development to determine mosquito transmission blocking activity. Finally, compounds with a strong inhibitory effect on both transmission stages were assessed on asexual stage parasite growth. **(B)** Screening strategy of pathogen box compounds on *P. falciparum* sporozoite motility. Freshly isolated *P. falciparum* sporozoites were pre-incubated with pathogen box compounds at 1 µM for 30 minutes, then added to plates and allowed to glide for 1 h in the continued presence of the compound. Trails were visualized by immunofluorescence staining of the circumsporozoite protein (CSP) trails left behind on plates and quantified by high-content imaging of 25 positions in each well. **(C-F)** Validation of the *P. falciparum* motility assay. *P. falciparum* sporozoites were pre-incubated with 0.1 to 10 µg/ml of mAb 2A10 (C&D) or 0.1 to 10 µM Cytochalasin D (E&F) for 30 minutes and added to wells for 1 h in the continued presence of the inhibitor. Sporozoites and trails were then stained for CSP and quantification of the area occupied by fluorescent staining was performed. Panels C&E: Representative images of CSP-stained sporozoites and trails when sporozoites are pre-incubated with the indicated concentrations of mAb 2A10 (C) or Cytochalasin D (E). Scale bars, 50 µm. Panel D&F: Quantification of the area occupied by CSP-stained sporozoites and trails in the indicated treatment groups. Imaging was performed on 25 positions per well with each dot representing the area occupied by fluorescent trails in one image. Data were pooled from 3 independent experiments and all conditions were compared to each other (Kruskal-Wallis test followed by Dunn's test, **** $P < 0.0001$, * $P < 0.05$, ns $P > 0.05$). Red bars indicate the mean.

A

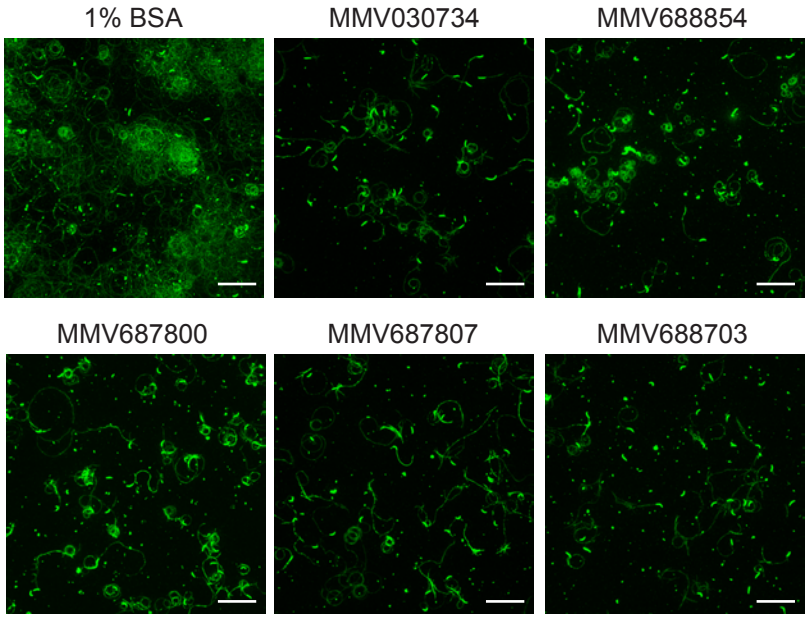

B

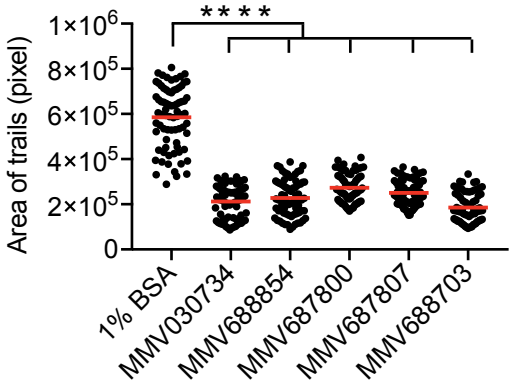

C

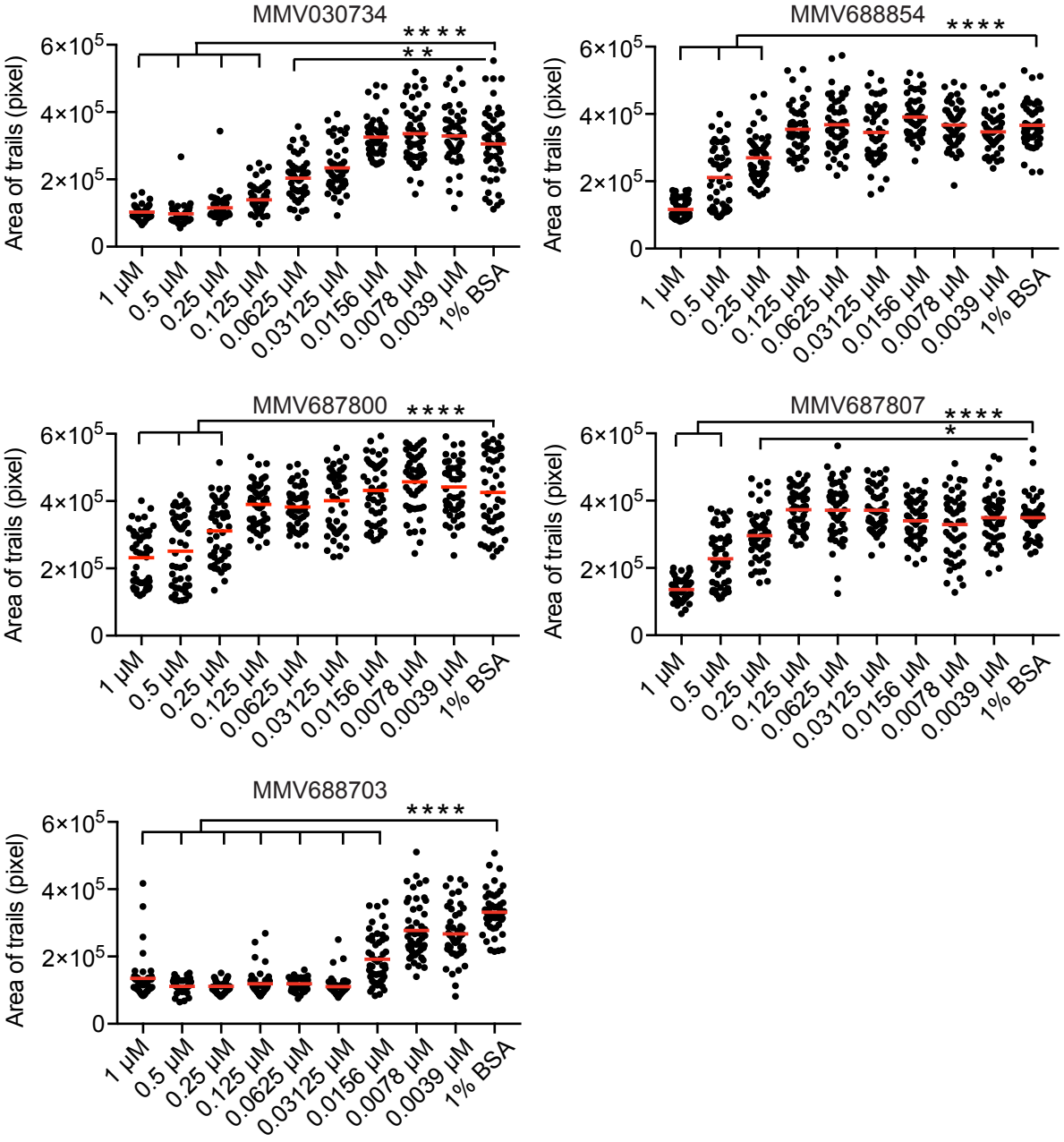

Figure 2. Five pathogen box compounds significantly reduce *P. falciparum* sporozoite motility

P. falciparum sporozoites were pre-incubated with the indicated compounds (MMV030734, MMV688854, MMV687800, MMV687807, MMV688703) for 30 minutes and allowed to glide in the continued presence of the compound for 1 h. Following this, sporozoites and trails were stained for CSP and the area occupied by fluorescent sporozoite and trails was quantified by high content imaging. **(A)** Representative images of CSP stained sporozoites and trails in the presence of each of the 5 inhibitory compounds. Scale bars, 50 μm **(B)** Quantification of area occupied by CSP-stained sporozoites and trails in the gliding assays. 25 images per well were analyzed with each dot representing data from one image. Data were pooled from 3 independent experiments and each inhibitor is compared to 1% BSA (Kruskal-Wallis test followed by Dunn's test, **** $P < 0.0001$). Red bars indicate the mean. **(C)** Dose-Response of the inhibitory pathogen box compounds. *P. falciparum* sporozoites were incubated with the indicated serially-diluted compounds MMV030734, MMV688854, MMV687800, MMV687807, or MMV688703 and the area occupied by CSP stained trails was quantified. 25 images per well were analyzed with each dot representing data from one image. Data were pooled from 2 independent experiments and serially-diluted compounds were compared to 1% BSA (Kruskal-Wallis test followed by Dunn's test, **** $P < 0.0001$, ** $P < 0.005$, * $P < 0.05$). Red bars indicate the mean.

A

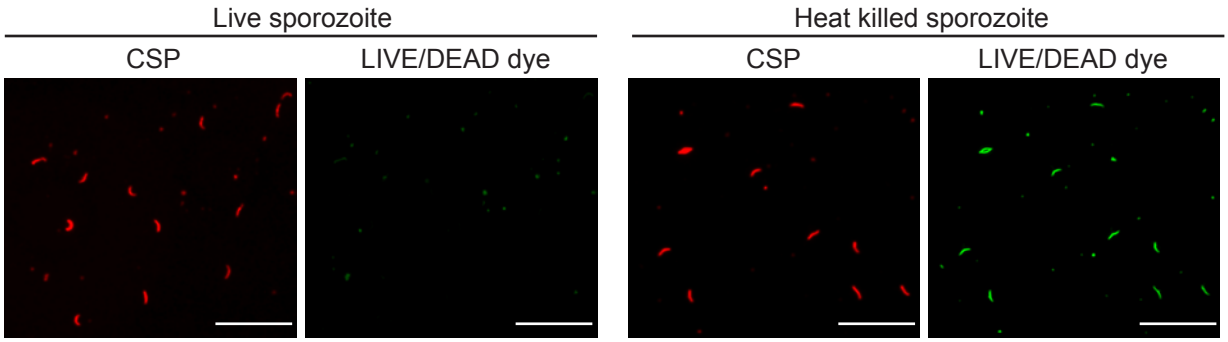

B

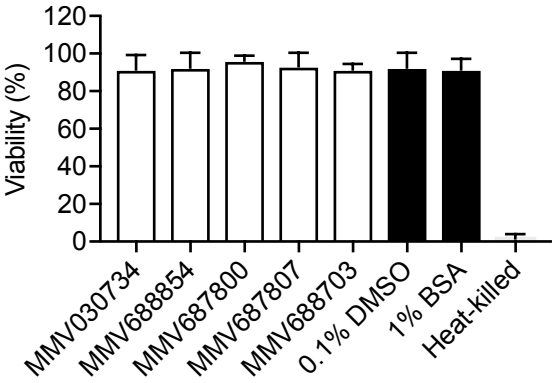

Figure 3. *P. falciparum* sporozoite viability after treatment with each of the five active pathogen box compounds. *P. falciparum* sporozoites were incubated with a fixable live/dead stain and the indicated pathogen box compound for 30 minutes at 20 °C and then moved to 37 °C for 1 h in the continued presence of the stain and compound. Following this, sporozoites were fixed, stained with antibodies specific for CSP, and quantified by immunofluorescence microscopy. **(A)** Representative images of sporozoite stained for CSP (red) and live/dead stain (green). Scale bars, 50 µm. **(B)** Quantification of sporozoite viability after treatment with compounds. Total sporozoites (CSP, red) and those that stained with the live/dead stain (green) were counted to determine percent viability (n ≥ 100 sporozoites per condition). Bars representing control samples are shown in black. Shown is the mean +/- standard deviation of two independent experiments.

Figure 4

A

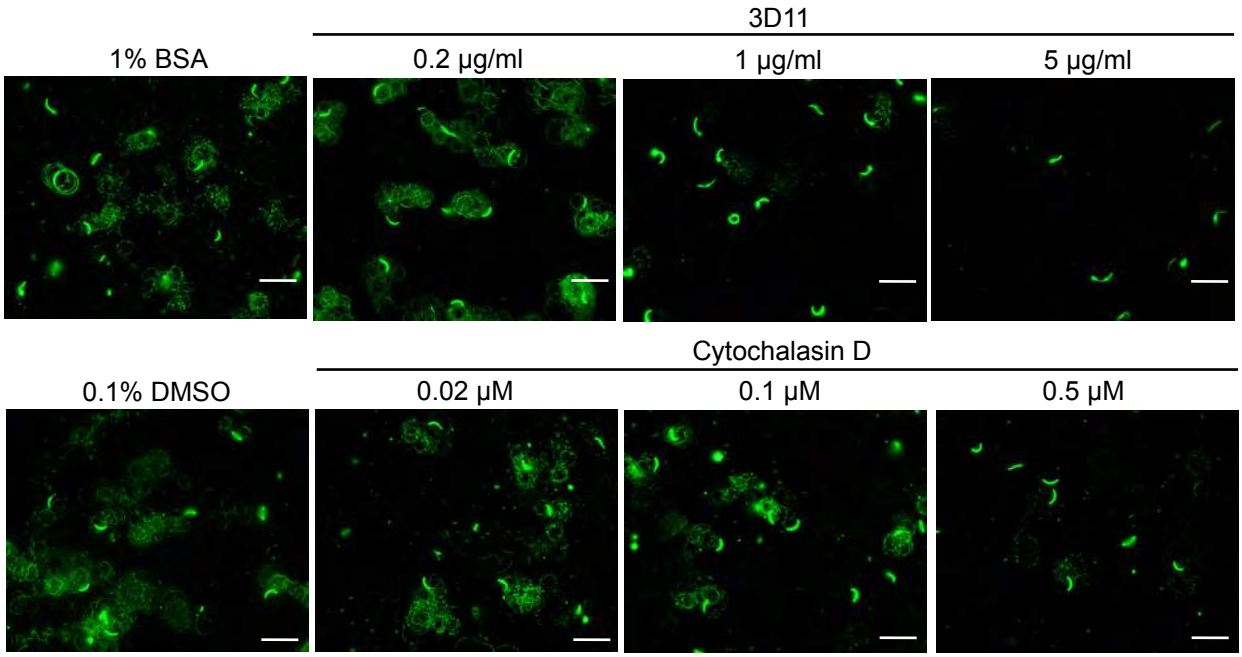

B

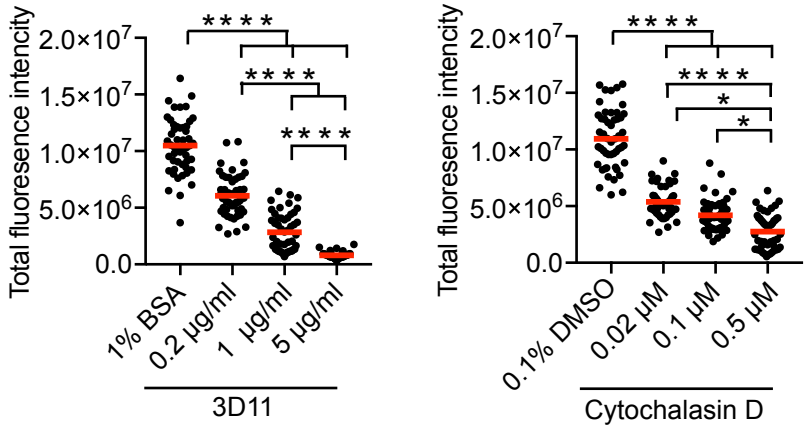

C

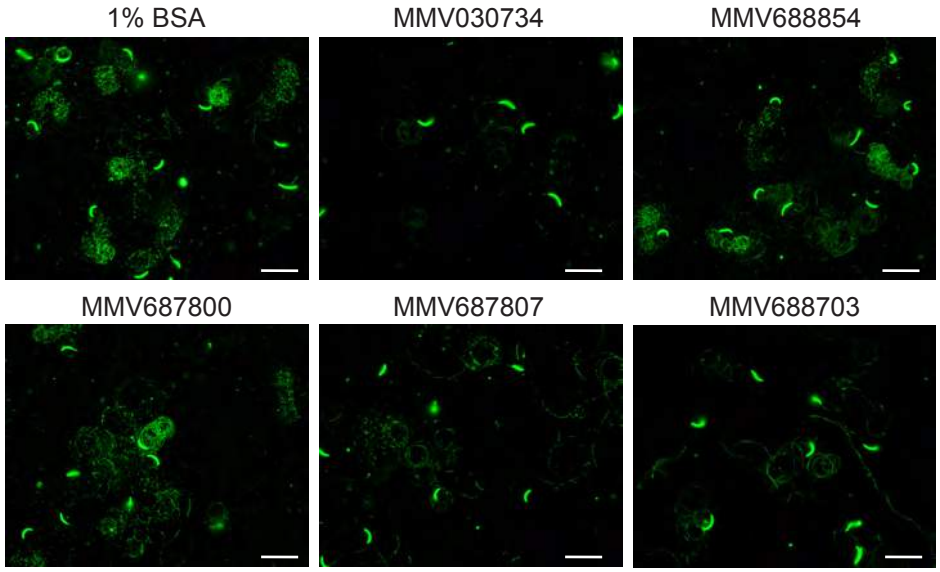

D

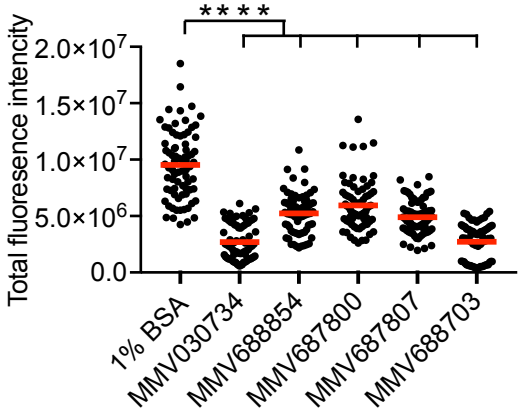

Figure 4. Testing the pathogen box inhibitory compounds on *Plasmodium berghei* sporozoite motility

(A&B) Validation of the *P. berghei* sporozoite motility assay. Sporozoites were pre-incubated with the indicated concentration of mAb 3D11 or Cytochalasin D for 30 minutes and then allowed to glide for 1 h in the continued presence of antibody or Cytochalasin D. Sporozoites and trails were stained for CSP and total fluorescence intensity of sporozoites and trails were quantified by Image J. Representative images of CSP-stained sporozoites and trails are shown in panel A. Scale bars, 20 μm. Panel B shows quantification of the total fluorescence intensity of CSP-stained sporozoites and trails for each treatment group. 25 images were acquired per well with each dot representing fluorescence intensity from one image. Data are pooled from 2 independent experiments and all conditions were compared to each other (Kruskal-Wallis test followed by Dunn's test, **** $P < 0.0001$, * $P < 0.05$). Red bars indicate the mean. **(C&D)** Testing of inhibitory pathogen box compounds on *P. berghei* sporozoites. Sporozoites were pre-incubated with 1 μM of each of the five inhibitory pathogen box compounds (MMV030734, MMV688854, MMV687800, MMV687807, MMV688703) for 30 minutes, then added to plates and allowed to glide for 1 h in the continued presence of the compound. Sporozoites and trails were stained for CSP and fluorescence intensity of sporozoites and trails were quantified by Image J. Representative images of CSP stained sporozoites and trails incubated with the indicated pathogen box compound are shown in panel C. Scale bars, 20 μm. Shown in panel D is quantification of the fluorescence intensity of CSP-stained sporozoites and trails in the presence of the indicated compound. 25 images per well were acquired with each dot representing the fluorescence intensity of one image. Data were pooled from 3 independent experiments and each inhibitor is compared to 1% BSA (Kruskal-Wallis test followed by Dunn's test, **** $P < 0.0001$). Red bars indicate the mean.

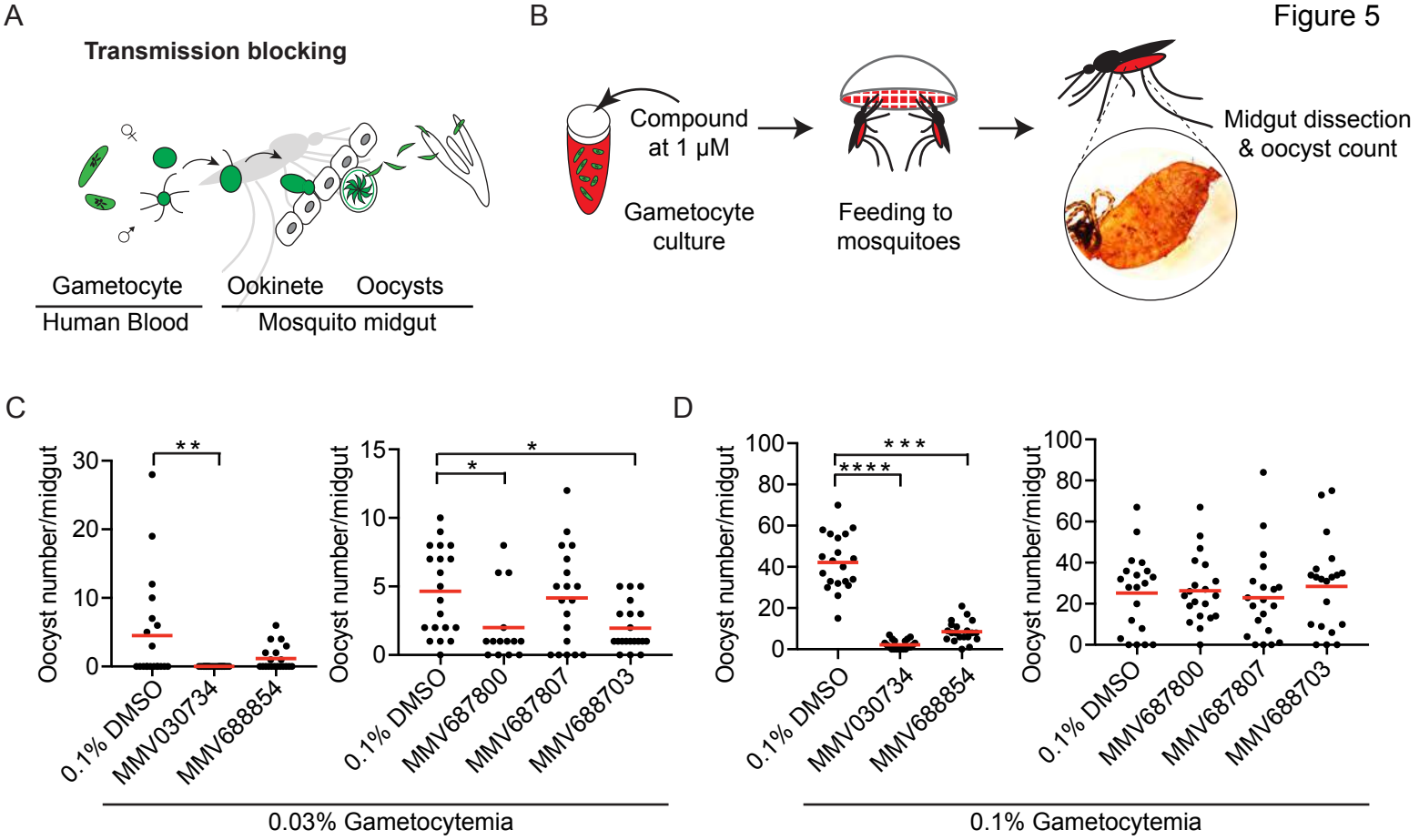

Figure 5. Testing the pathogen box inhibitory compounds for mosquito transmission blocking activity

(A) Schematic representation of *Plasmodium* transmission to the mosquito. **(B)** Schematic representation of assay set up. The mature gametocyte culture is mixed with each compound to a final concentration of 1 µM and fed to *An. stephensi* mosquitoes. Nine days later, mosquito midguts were dissected and oocysts were counted. **(C&D)** *An. stephensi* mosquitoes were fed a blood meal of either 0.03% (C) or 0.1% (D) gametocytemia in the presence of the indicated compound or DMSO control. On day 8 post-blood meal, individual mosquitoes were dissected and oocysts were counted for 15 to 20 mosquitos per group. Each group is compared to DMSO control (Kruskal-Wallis test followed by Dunn's test, **** $P < 0.0001$, *** $P < 0.0005$, ** $P < 0.005$, * $P < 0.05$). Red bars indicate the mean.

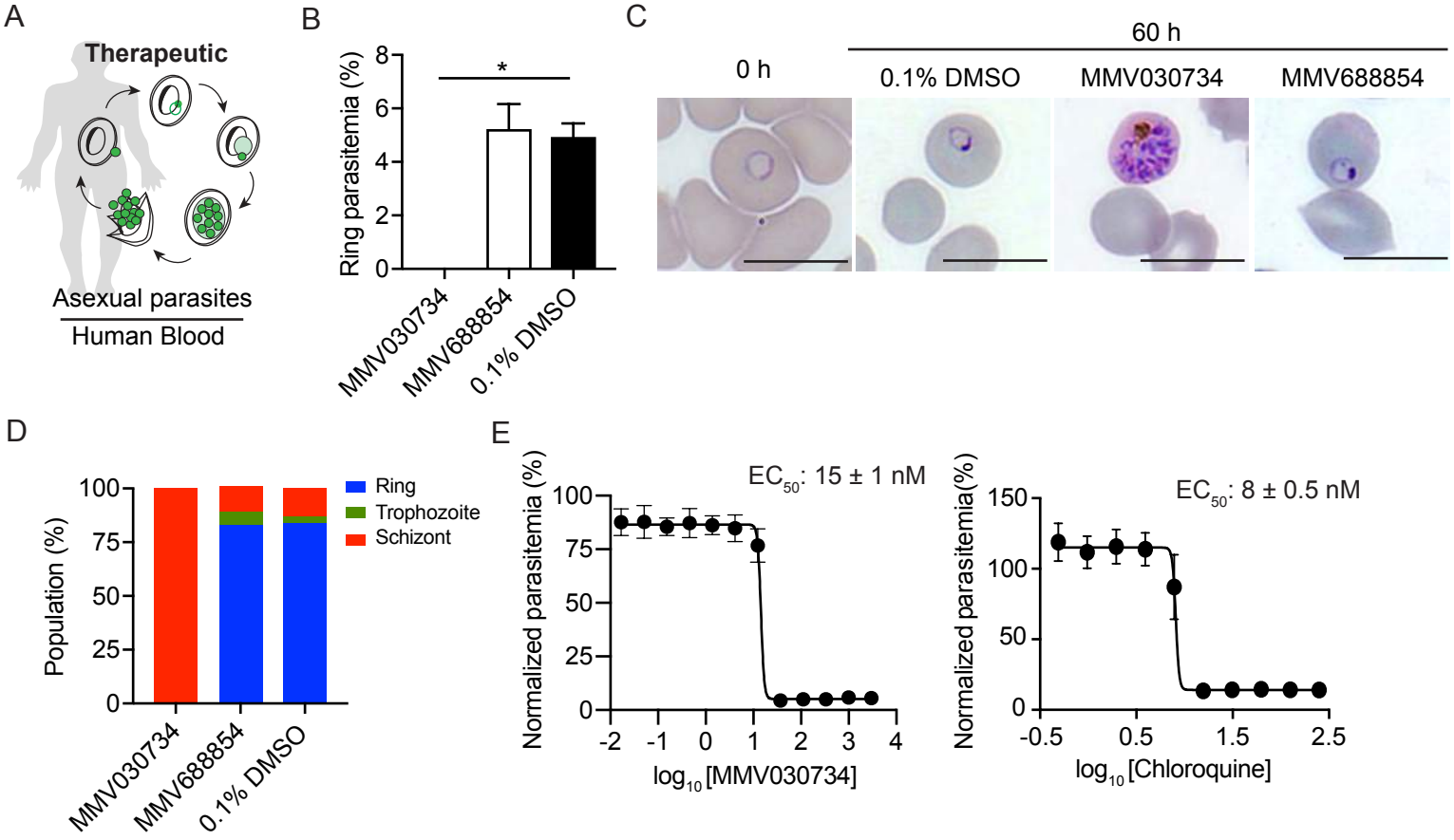

Figure 6. Pathogen box compound MMV030734 reduces asexual stage parasite growth and inhibits egress.

(A) Schematic representation of *Plasmodium* asexual blood stage cycle. **(B)** Quantification of ring stage parasitemia. Synchronized *P. falciparum* ring stage parasites were incubated with compound MMV030734 or MMV688854 at 1 μM or 0.1% DMSO for 60 h at which point Giemsa-stained blood smears were made and ring stage parasites were counted. The mean +/- standard deviation is shown from two technical replicates. ANOVA multiple comparisons, *P<0.01. **(C)**. Representative images of Giemsa-stained asexual stage parasites at 0 h and at 60 h in the indicated treatment group. Scale bar, 10 μm. **(D)** Giemsa-stained blood smears taken at 60 h were scored based on the number of ring, trophozoite, and schizont stage parasites. The percentage of each lifecycle stage is shown for one hundred infected erythrocytes from each treatment group. **(E)** Dose-response plot for parasites grown in presence of MMV030734 or Chloroquine for 72 h. Data were pooled from two biological replicates each with four technical replicates. The mean parasitemias ± standard deviation (SD) are shown normalized to the DMSO control. Half maximal effective concentration (EC_{50}) is represented as mean ± SD.

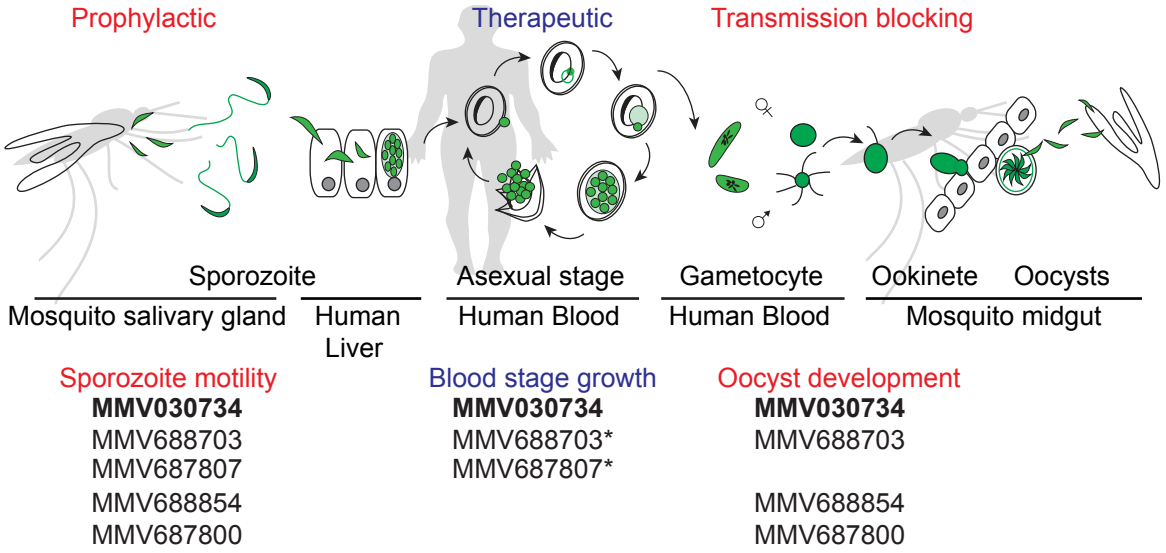

Figure 7. Summary of the five motility-inhibitory compounds across the *Plasmodium* life cycle

Pathogen box compounds were screened for their impact on *P. falciparum* sporozoite motility and 5 compounds (MMV030734, MMV688854, MMV687800, MMV687807, MMV688703) showed significant inhibition in this assay. Of these compounds, MMV030734 and MMV68854 inhibited transmission of *P. falciparum* gametocytes to the mosquito at high gametocytemia and MMV687800 and MMV688703 inhibited transmission only at low gametocytemia. MMV030734, MMV687807 and MMV688703 had a significant inhibitory effect on asexual blood stage growth. Thus, two compounds, MMV030734 and MMV688703 inhibited all three *P. falciparum* life cycle stages. *Blood stage inhibitory effect of MMV688703 and MMV687807 was confirmed by Duffy. S et al (15).

Sup Figure 1

A

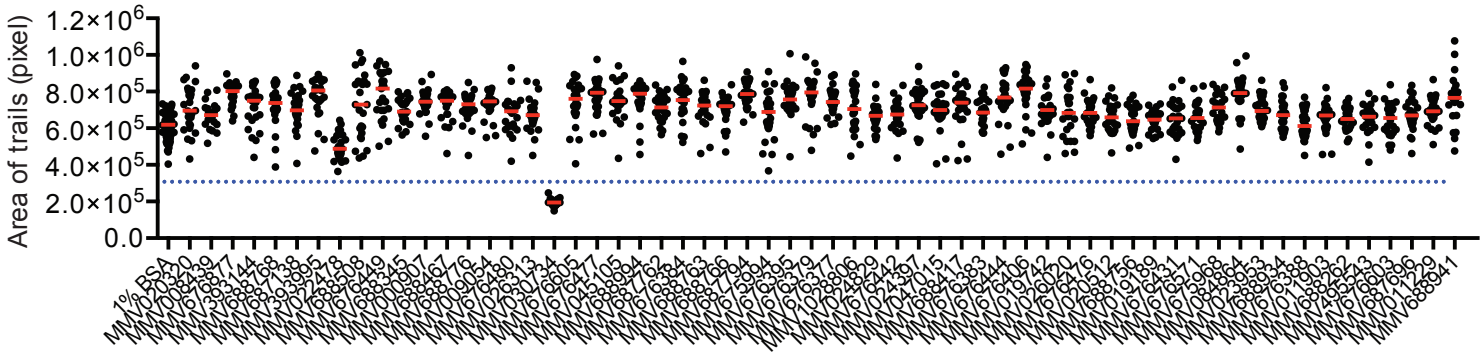

B

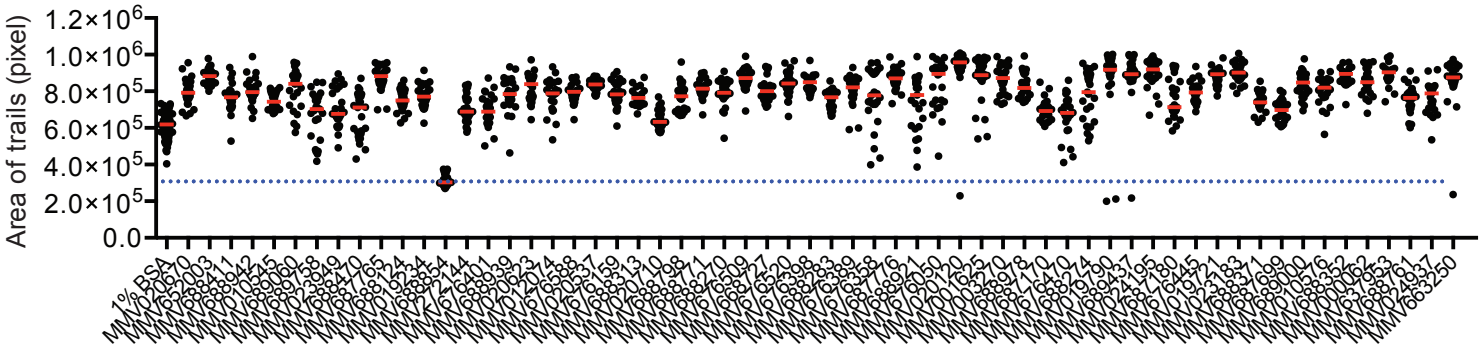

C

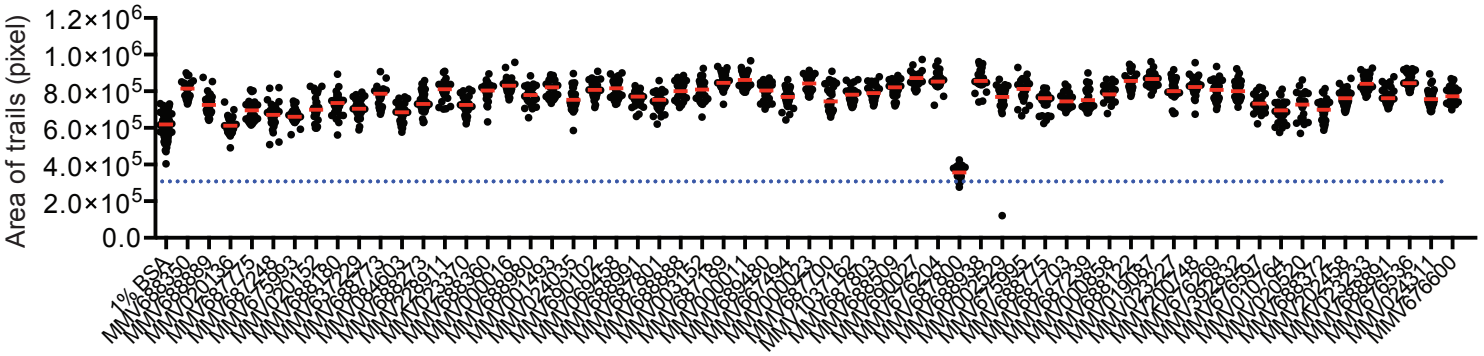

D

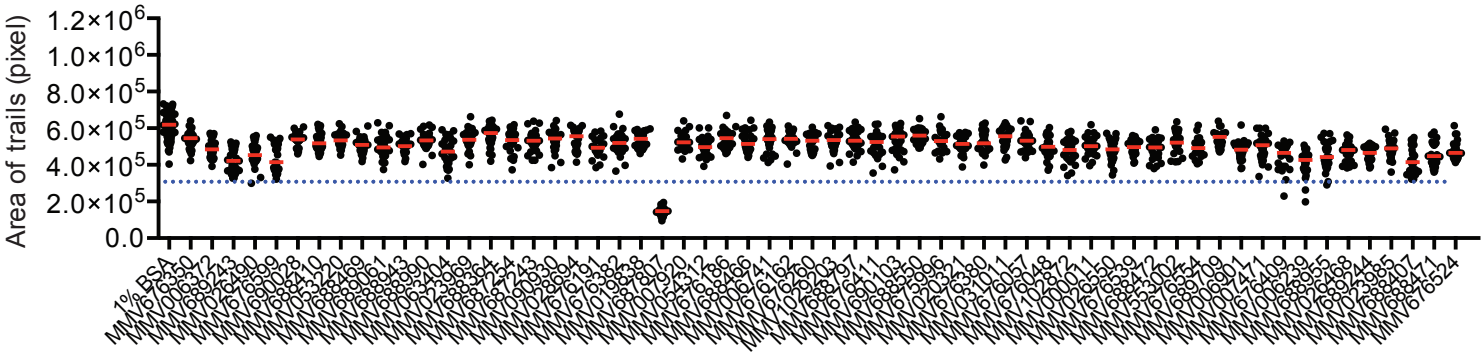

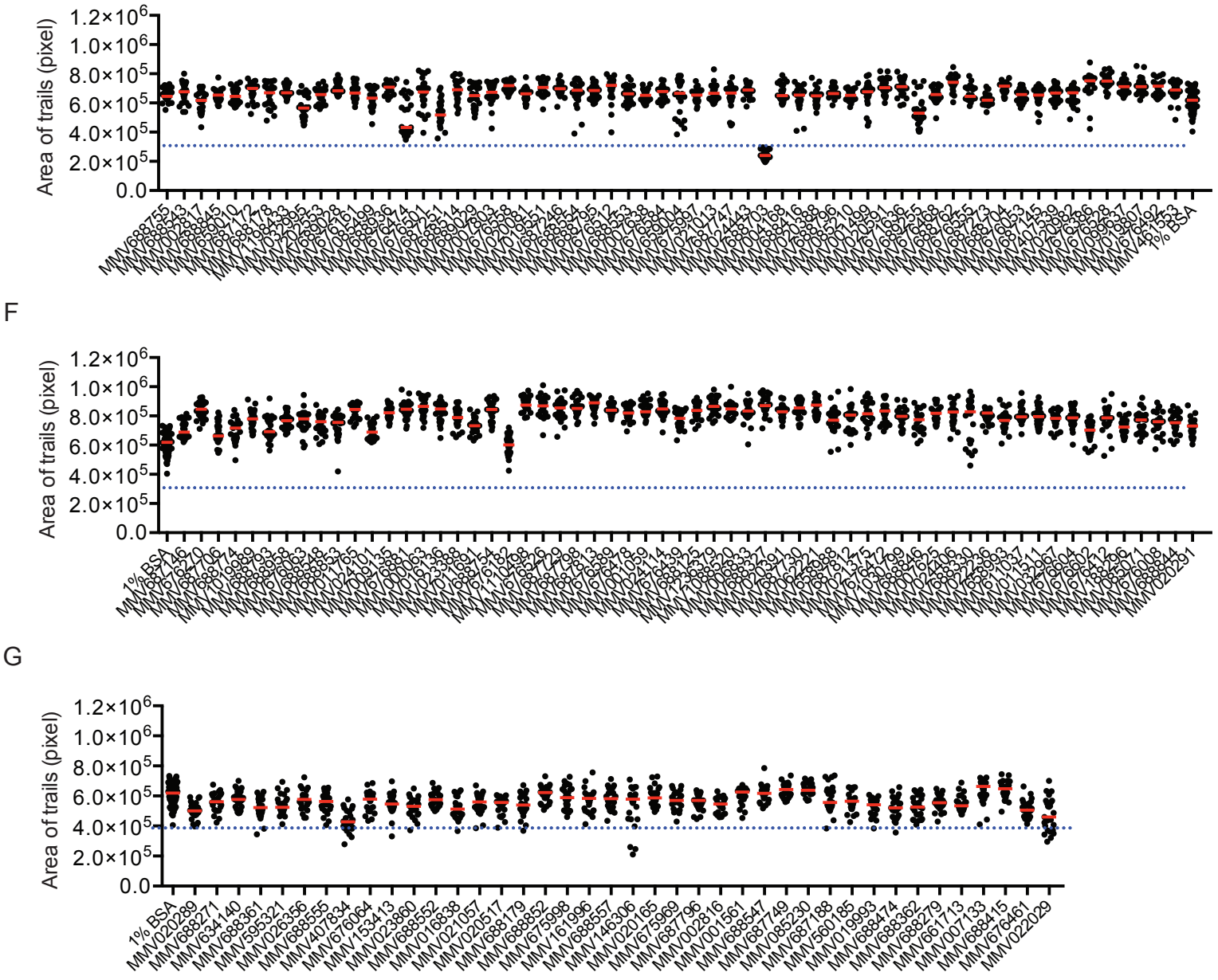

Supplemental Figure 1. Screening of pathogen box compounds on *P. falciparum* sporozoite motility

Freshly isolated *P. falciparum* sporozoites were incubated with each of the 400 pathogen box compounds at 1 µM and allowed to glide for 1 h. CSP trails were stained and quantification of the area occupied by the trails was performed. Red bars indicate the mean area occupied by trails. Each panel shows a different subset of the 400 compounds. Inhibition of motility was observed in sporozoites treated with MMV030734 (panel A), MMV688854 (panel B), MMV687800 (panel C), MMV687807 (panel D), MMV688703 (panel E). The dotted line in each graph indicates the threshold for identifying a compound hit. The threshold is half of the mean area occupied by the trails of parasites in 1% BSA.

Table 1. Effect of five compounds in Plasmodium life cycle and potential targets

	MMV030734	**MMV688854**	**MMV687800**	**MMV687807**	**MMV688703**
Target organism in the Pathogen box	Malaria	Cryptosporidium	Reference compound: Clofazimine	Mycobacterium Tuberculosis	Toxoplasma
Potential target	PfCDPK1	TgCDPK1 (PfCDPK4)			cGMP dependent protein kinase
Results (from this study)					
***P. falciparum* sporozoite motility**	Significant inhibition at 0.0625 µM	Significant inhibition at 0.25 µM	Significant inhibition at 0.25 µM	Significant inhibition at 0.25 µM	Significant inhibition at 0.0156 µM
***P. berghei* sporozoite motility**	72% inhibition at 1 µM	45% inhibition at 1 µM	38% inhibition at 1 µM	49% inhibition at 1 µM	71% inhibition at 1 µM
***P. falciparum* oocyst formation**	Significant inhibition at 1 µM with 0.1% gametocytemia	Significant inhibition at 1 µM with 0.1% gametocytemia	Significant inhibition at 1 µM with 0.03% gametocytemia	No effect on Oocyst development	Significant inhibition at 1 µM with 0.03% gametocytemia
***P. falciparum* asexual stage growth**	EC_{50}: 15±1 nM Schizont egress defect was observed	Inactive	No data	No data	No data
MMV data sheet					
***P. bergehi* liver stage development, IC50 determination by luciferase assay**	100% inhibition at 10 µM IC_{50}: 0.32 µM	No data	No data	No data	No data
***P. falciparum* asexual stage growth**	3D7: IC_{50} 0.41 µM DD2: IC_{50} 0.2 µM W2: IC_{50} 1.1 µM	No data	No data	No data	No data
***P. falciparum* (NF54) inhibition of late-stage gametocyte (IV-V) development**	9% inhibition at 10 µM	No data	No data	No data	No data
Cytotoxicity **CC_{20} and CC_{50}: Cytotoxic concentration of the compounds to cause death of 20% and 50% of viable cells**	HepG2 CC_{20}: 5.8 µM CC_{50}: >10 µM	HepG2 CC_{20}: 22.6 µM	HepG2 CC_{20}: 6.6 µM	HepG2 CC_{50}: 0.7 µM	HepG2 CC_{20}: 2.7 µM HL60 CC_{50}: > 50 µM
S. Duffy et al, 2017					
***P. falciparum* asexual stage growth**	3D7: IC_{50} < 5 µM	3D7: IC_{50} > 20 µM	84% inhibition at 20 µM (3D7) Inactive (NF54)	3D7: IC_{50} 1.82 µM	3D7: IC_{50} 3.16 µM
***P. falciparum* inhibition of late-stage gametocyte (IV-V) development**	IC_{50} 5-10 µM	IC_{50} 5-10 µM	Inactive	IC_{50} 5.07 µM	IC_{50} >20 µM